

Final Ti Model Results

Tigany Zarrouk

January 13, 2020

Contents

1	Objective Function	2
2	Defect Clusters	4
2.1	Octahedral O interstitial relaxation	4
2.2	Tetrahedral O interstitial relaxation	5
2.3	Energies for defects	7
2.4	All formation energies	10
3	Gamma surfaces	11
3.1	Basal	12
3.2	Prismatic	12
3.3	Pyramidal first order	14
3.4	Data	15
4	Dislocation core structures	16
4.1	Methodology	16
4.2	Discussion	16
4.3	TODO Dissociation Distance Analysis	17
4.3.1	Analysis with Final Ti model.	18
4.4	TODO Disregistry Analysis	18
4.5	IP1	20
4.6	IP2	21
4.7	IP3	22
4.8	IP4	23
4.9	IP5	24
4.10	Ghazisaeidi Results for comparison	25
4.11	Peierls Stress	25
4.11.1	Applying strain	25

4.11.2	xz Strain	26
4.11.3	xy strain	27
4.11.4	Pyramidal Strain	29
4.12	Data	29
4.13	Directory of the results	29
5	Binding energies to dislocations	29
6	BOP	30
6.1	4 recursion levels	30
7	Bibliography	31

1 Objective Function

PARAMETERS fdd=0.1958363809 qdds=0.5591275855 qddp=0.5690351902
qddd=0.7745947522 b0=58.0906936439 p0=1.2185323579 b1=-3.2299188646
p1=0.6862915307 b2=593519.1134129359 m2=-11.5000000000 p2=0.0000000000
ndt=2.0000000000 cr1=-6.0000000000 cr2=3.0474400934 cr3=-1.2317472193
r1dd=6.5000000000 rcdd=10.0000000000 rmaxhm=10.1000000000 npar=18
VARGS -vfdd=0.1958363809 -vqdds=0.5591275855 -vqddp=0.5690351902 -
vqddd=0.7745947522 -vb0=58.0906936439 -vp0=1.2185323579 -vb1=-3.2299188646
-vp1=0.6862915307 -vb2=593519.1134129359 -vm2=-11.5000000000 -vp2=0.0000000000
-vndt=2.0000000000 -vcr1=-6.0000000000 -vcr2=3.0474400934 -vcr3=-1.2317472193
-vr1dd=6.5000000000 -vrcdd=10.0000000000 -vrmaxhm=10.1000000000

Quantity	From Model	Target
a _{hcp}	5.58523112	5.57678969
c/a	1.58371266	1.58731122
a _{omega}	8.93475285	8.73254342
c _{omega}	5.38726911	5.32343103
a _{4h}	5.57584691	5.56325146
c _{4h}	18.09810672	17.75908031
a _{6h}	5.57365569	5.54639384
c _{6h}	27.18378460	26.77136353
a _{bcc}	6.20079768	6.17948863
a _{fcc}	7.87290654	7.88677000
DE(o,h)	0.58764167	-0.63343333
DE(4h,h)	1.58019500	3.17160000
DE(6h,h)	2.48264833	3.72005000
DE(b,h)	5.35128500	7.63520000
DE(f,h)	3.78088500	4.51880000
c ₁₁	171.60928873	176.10000000
c ₃₃	198.90063708	190.50000000
c ₄₄	47.42549704	50.80000000
c ₁₂	94.65941969	86.90000000
c ₁₃	61.22624060	68.30000000
M _{freq0}	2.59341377	2.85858719
M _{freq1}	2.59341378	2.85858719
M _{freq2}	2.59341378	2.85858719
M _{freq3}	2.59341379	2.85858719
M _{freq4}	5.85272461	5.66706047
M _{freq5}	5.85272461	5.66706047
H _{freq0}	3.82320403	4.80643423
H _{freq1}	3.82320403	5.58010025
H _{freq2}	6.40288977	5.65316738
H _{freq3}	6.40288977	6.36651842
H _{freq4}	7.92857431	6.40050186
H _{freq5}	7.92857431	7.64082373
bandw. G	3.69394702	5.87085872
bandw. K	4.65178817	4.97424321
bandw. M	5.19329495	7.78109872
bandw. L	4.21232412	6.34433701
bandw. H	3.54700549	9.70902614
DOSerr _h	0.00000000	0.00000000
DOSerr _o	0.00000000	0.00000000
E _{prisf}	98.95340236	220.00000000

———— E_{prismaticfault} ————

tbe:	98.953	mJ/m ²	
DFT:	250.000	mJ/m ²	[Benoit 2012]
DFT:	233.000	mJ/m ²	[Ackland 1999]

———— E_{Basalfault} I2 ————

tbe:	211.658	mJ/m ²	
DFT:	260.000	mJ/m ²	[Benoit 2012]

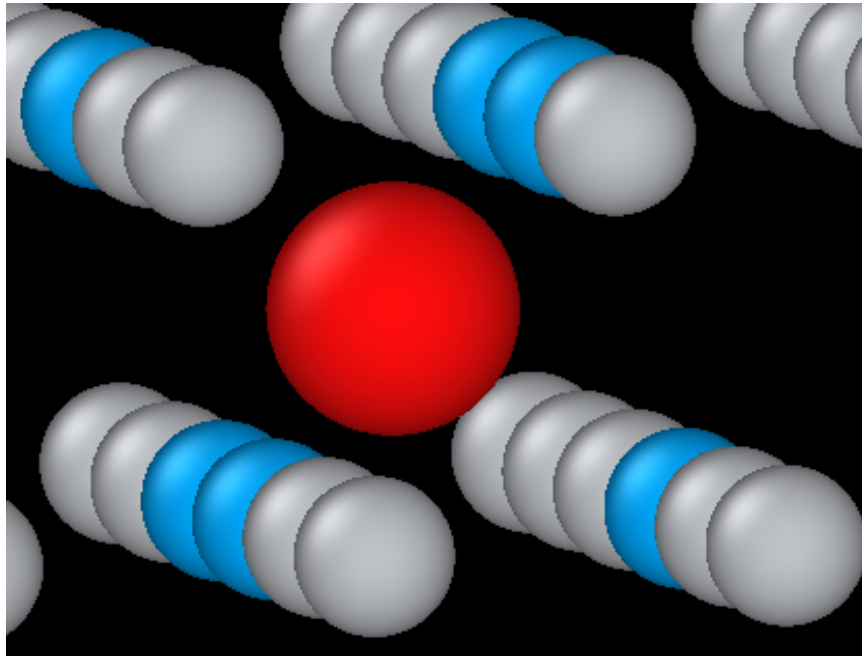
2 Defect Clusters

———— E_{vacancyformation} ————

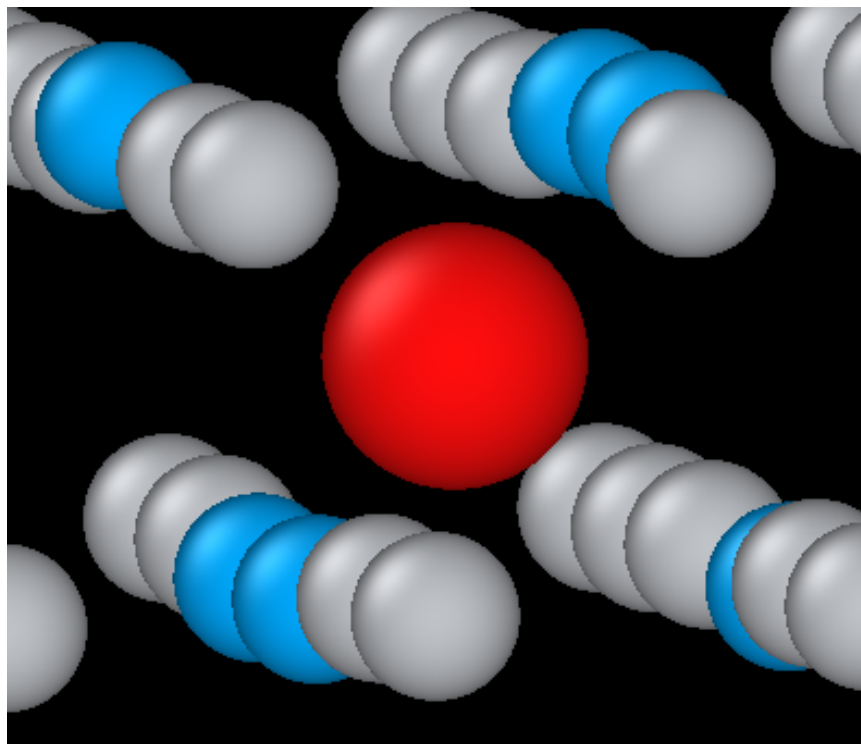
tbe:	2.347	eV	
DFT:	1.950	eV	GGA-PAW: Angsten (2013)
exp:	1.270	eV	Hashimoto (1984)

2.1 Octahedral O interstitial relaxation

Initial:

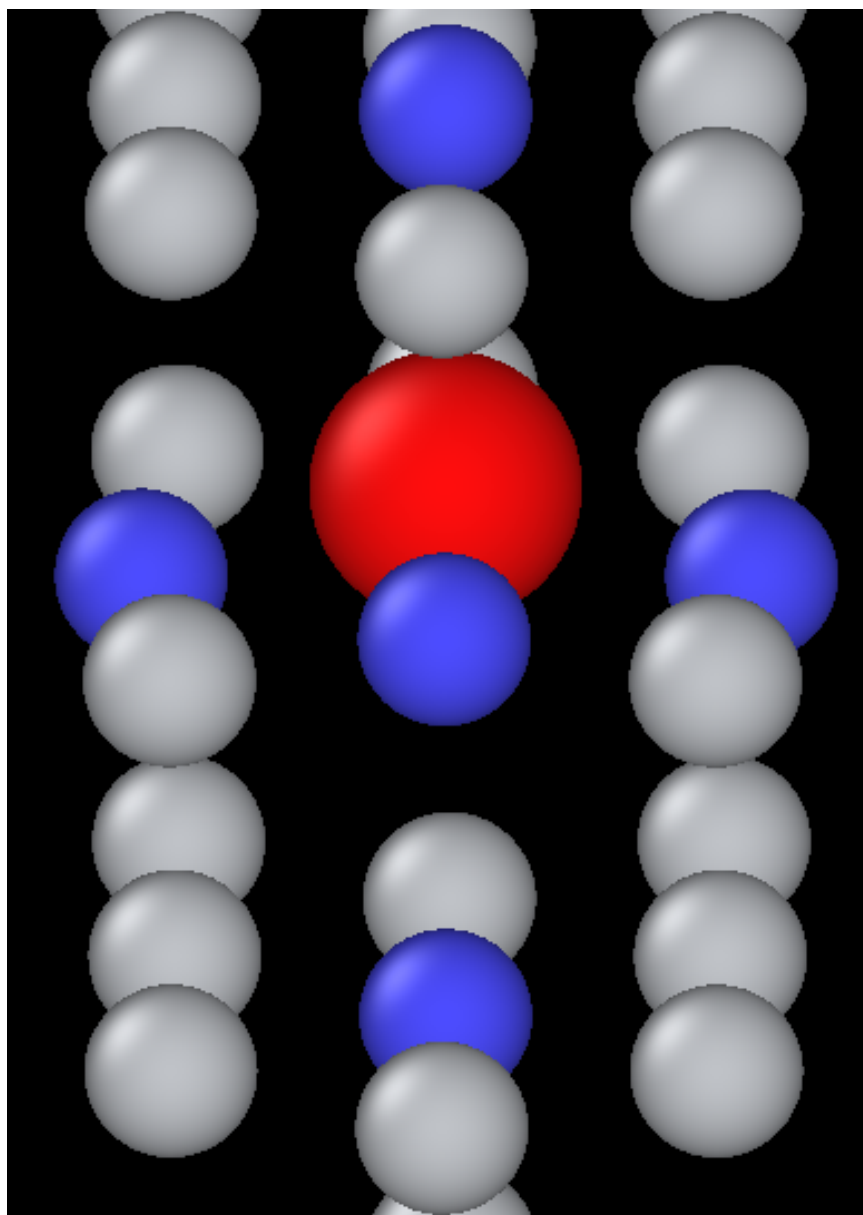


Final:

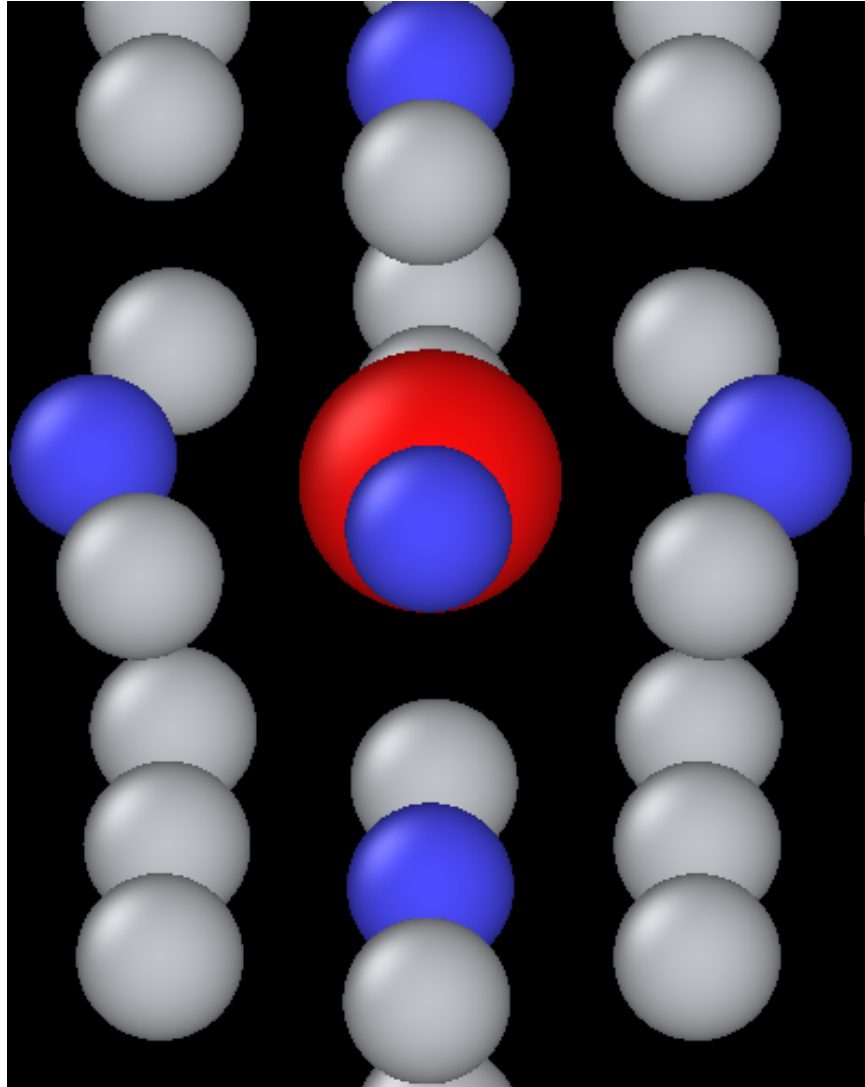


2.2 Tetrahedral O interstitial relaxation

Initial:



Final:



2.3 Energies for defects

Relative differences are

» $(E_{\text{tetrahedral}} - E_{\text{octahedral}})$

tbe:	1.65 eV	
GGA-DFT:	1.23 eV	Kwasniak (2013)

» $(E_{\text{hexahedral}} - E_{\text{octahedral}})$

tbe: 0.90 eV

> Note: Preference for tetrahedral oxygen to go into hexahedral site as seen by images above

All formation energies below use the chemical potential of Akysanov (2013) of value $\mu_{\text{oxygen}} = \frac{5.6}{2} eV$.

2.4 All formation energies

Quantity	Energy (eV)
E_{Vf}	2.347
E_{Tsol}	- 21.783
$E_{Tdilimp}$	- 28.991
$E_{Tformation}$	- 21.783
$E_{TVformation}$	- 18.905
$E_{Tvacsolbind}$	- 0.530
E_{Osol}	- 23.436
$E_{Odilimp}$	- 30.645
$E_{Oformation}$	- 23.436
$E_{OVformation}$	- 18.905
$E_{Ovacsolbind}$	- 2.183
E_{OOSol}	- 49.606
$E_{OODilimp}$	- 56.814
$E_{OOformation}$	- 46.806
$E_{OOVformation}$	- 41.910
$E_{OOvacsolbind}$	- 2.547
E_{OOOSol}	- 76.037
$E_{OOOdilimp}$	- 83.246
$E_{OOOformation}$	- 70.437
$E_{OOOVformation}$	- 66.013
$E_{OOOvacsolbind}$	- 2.076
$E_{OOOOSol}$	- 102.470
$E_{OOOOdilimp}$	- 109.679
$E_{OOOOformation}$	- 94.070
$E_{OOOOVformation}$	- 88.998
$E_{OOOOvacsolbind}$	- 2.724
$E_{OOOOOSol}$	- 128.781
$E_{OOOOOdilimp}$	- 135.989
$E_{OOOOOformation}$	- 117.581
$E_{OOOOOVformation}$	- 113.649
$E_{OOOOOvacsolbind}$	- 1.583
$E_{OOOOOOSol}$	- 155.148
$E_{OOOOOOdilimp}^{10}$	- 162.357
$E_{OOOOOOformation}$	- 141.148
$E_{OOOOOOVformation}$	- 137.110
$E_{OOOOOOvacsolbind}$	- 1.690

3 Gamma surfaces

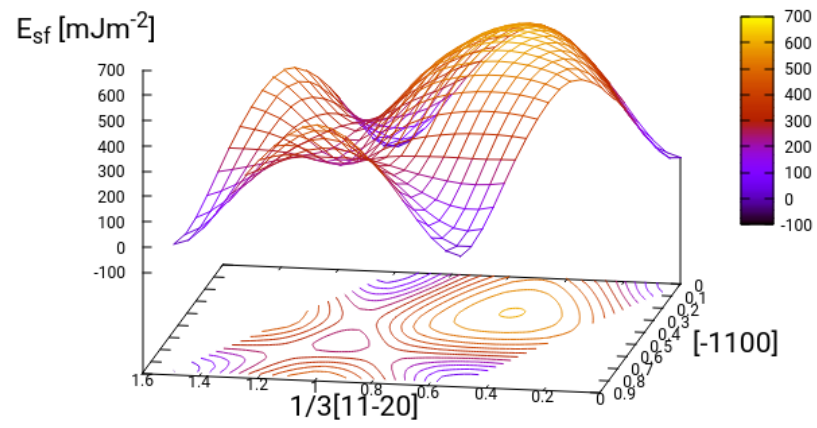
Energies are accurate to within 2 mJm^{-2} , comparing the energies of points in the corners which (the zeros of energy). So surface energies might be $\pm 2 \text{ mJm}^{-2}$ off which is reasonable.

These calculations were done in tight binding with 15 layers for both basal and prismatic with k-points adjusted accordingly. DFT comparisons are used results of Rodney.

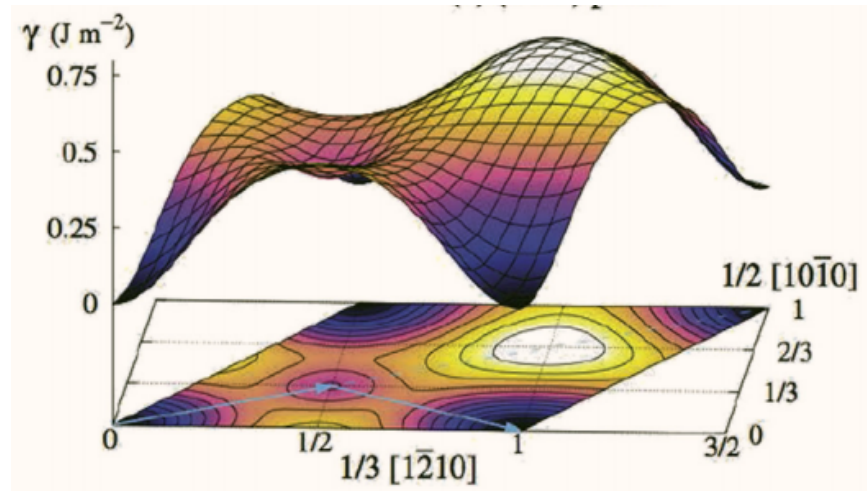
The Pyramidal surface was obtained using the same 32 atom cell that Ready used in his paper on the pyramidal gamma surface with DFT pseudopotentials.

3.1 Basal

TBE:

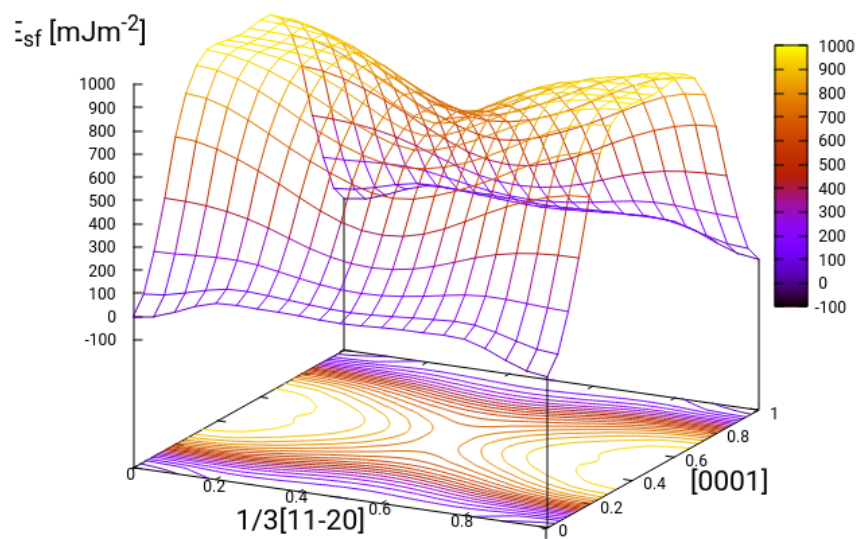


DFT:

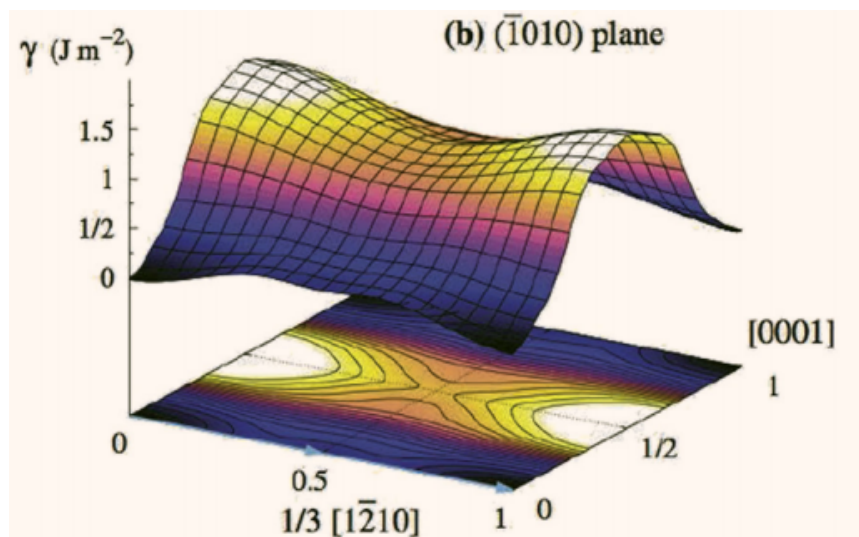


3.2 Prismatic

TBE:

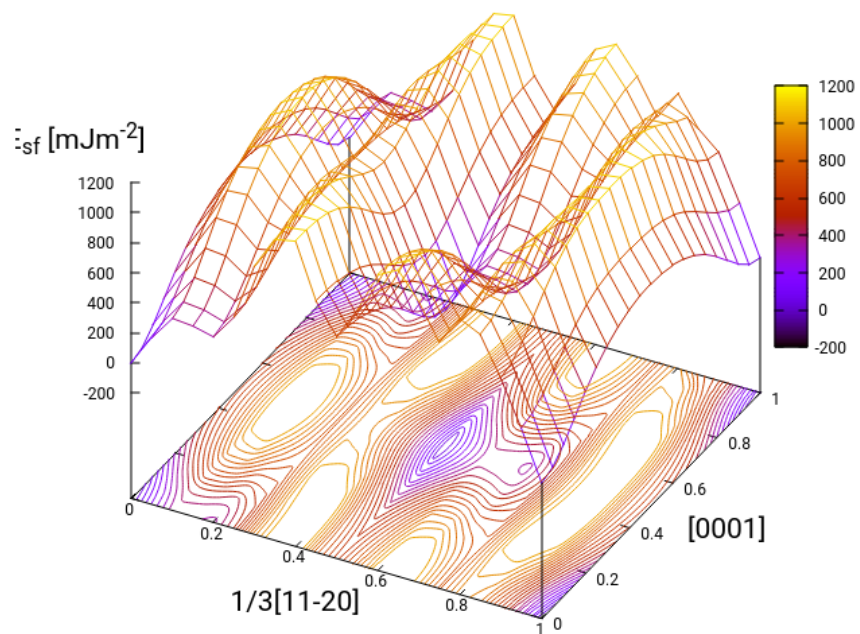


DFT:

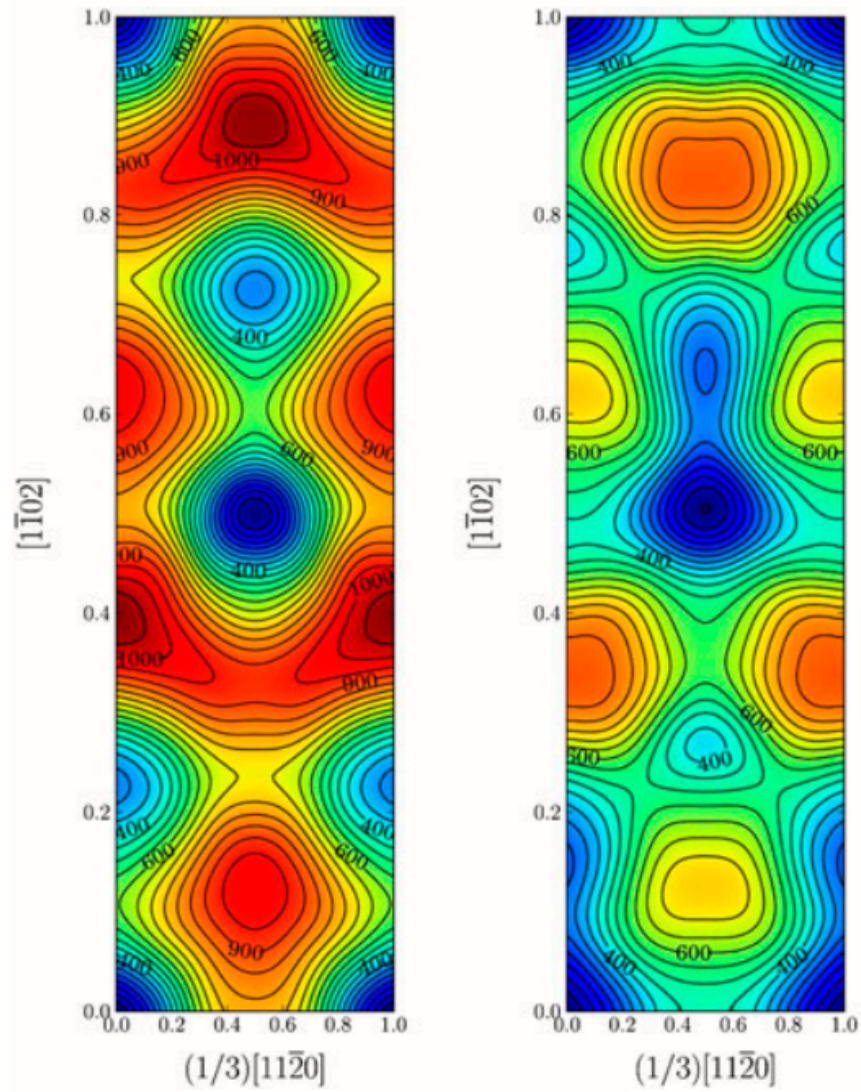


3.3 Pyramidal first order

TBE:



DFT pseudopot:



3.4 Data

basal_{gsdata} prismatic_{gsdata} pyramidal_{gsdata}

4 Dislocation core structures

4.1 Methodology

In the following, we see results of dislocation relaxation. The partial differential displacement maps are of dislocations in their initial and final states in different initial positions. The atoms were relaxed until the root-mean square force acting on each atom was less than 1×10^{-5} Ryd/Bohr.

These relaxations can be distinguished by the different initial positions of the dislocation centre (elastic centre) as following the paper by Tarrat [1].

The partial burger's vector seen here is the $1/6[11\bar{2}0]$ dislocation, and this is the Burger's vector plotted on each of the initial positions.

4.2 Discussion

One can see that all of the dislocations have dissociated on the prismatic plane. But there is a difference between initial positions as to upon which prismatic plane they dissociate on, from the original.

Only initial position 2 actually dissociated on a different prismatic plane to the others.

The positions of the partials are also different once each of the separate initial positions have been relaxed.

IP2 and IP3, although they are on different planes, have a very similar core structure to each other. They are both asymmetric cores.

IP1 has the upper partial dislocation located within an adjacent triangle to the left, compared to IP2 and IP3. The lower partial has been shifted downwards, by one triangle down and to the right, with respect to IP3. The core structure of IP5 is indistinguishable from IP1. These cores can be deemed as metastable, as they have a slightly higher energy than the other cores.

The upper partial of IP4 has been displaced upwards by one Peierls valley with respect to IP3. The lower partial is in the same triangle as IP3. IP4 is a mirrored core.

Each of these cores are asymmetric, using the definition by Tarrat [1].

The energies for each of the dislocation cores, when relaxed to 1×10^{-5} Ryd/Bohr is

Initial position	E_{total}
1	-331.54658899
2	-331.54660063
3	-331.54660053
4	-331.54660061
5	-331.54658717

The

The dissociation distance is consistent between the different initial positions of the elastic centres. The distance is $\approx 4c = 35.4 \text{ Bohr} = 18.7$, this is double the distance seen in Ghazisaedi and Trinkle [2] and double the distance that is found in the DFT Zr results by Clouet [3].

4.3 TODO Dissociation Distance Analysis

Following [3], one can dislocation elasticity theory to compute the dissociation distance of a dislocation in both the basal and prism planes. The energy variation caused by a dissociation length d is

$$\Delta E_{\text{diss}}(d) = -b_i^{(1)} K_{ij} b_j^{(2)} \ln\left(\frac{d}{r_c}\right) + \gamma d,$$

where $\mathbf{b}^{(i)}$ are the burger's vectors of the dissociated dislocations. γ is the corresponding gamma surface energy and K is the Stroh matrix. Controlling the dislocation core radius and the dislocation elastic energy, one can find the equilibrium dissociation distance as

$$d^{\text{eq}} = \frac{b_i^{(1)} K_{ij} b_j^{(2)}}{\gamma}$$

With the orientation of the simulation cell as, $U_1 = na_{\frac{1}{2}}[10\bar{1}0]$, $U_2 = mc[0001]$, $U_3 = a_{\frac{1}{3}}[1\bar{2}10]$, one finds the components of the Stroh matrix as:

$$K_{11} = \frac{1}{2\pi}(\bar{C}_{11} + C_{13})\sqrt{\frac{C_{44}(\bar{C}_{11} - C_{13})}{C_{33}(\bar{C}_{11} + C_{13} + 2C_{44})}} \quad (1)$$

$$K_{22} = \sqrt{\frac{C_{33}}{C_{11}}} K_{11} \quad (2)$$

$$K_{33} = \frac{1}{2\pi}\sqrt{\frac{1}{2}C_{44}(C_{11} - C_{12})} \quad (3)$$

here, $\bar{C}_{11} = \sqrt{C_{11}C_{33}}$.

From the gamma surface, for the basal plane one expects a dissociation of $1/3[1\bar{2}10] = 1/3[1\bar{1}00] + 1/3[0\bar{1}10]$. Then dissociation length in the basal plane is given by

$$d_b^{\text{eq}} = \frac{(3K_{33} - K_{11})a^2}{12\gamma_b}$$

For the prism plane the $1/3[1\bar{2}10]$ dislocation can dissociate into $1/6[1\bar{2}10] \pm \alpha(c/a)[0001]$ where the parameter α controls the position of the stacking fault minimum along the $[0001]$ direction. Only in interatomic potentials like the EAM, do we find that $\alpha = 0.14$.

The dissociation length is

$$d_p^{\text{eq}} = \frac{(K_{33}a^2 - 4\alpha^2 K_{22}c^2)}{4\gamma_p}$$

4.3.1 Analysis with Final Ti model.

Using

$$d_p^{\text{eq}} = \frac{(K_{33}a^2 - 4\alpha^2 K_{22}c^2)}{4\gamma_p}$$

with $K_{33} = 6.79853 \text{ GPa} = 6.79853/160.21766208 = 0.042433087 \text{ eV}/\text{\AA}^3$, $\alpha = 0$ and $\gamma_p = 98.95340236 \text{ mJm}^{-2} = 1.6021766208 * 10^{(-19)} * 10^{-3} * 10^{20} * 98.95340236 = 1.58540827809 \text{ eV}/\text{\AA}^3$, $a = 2.955577$ we have the equilibrium dissociation distance in the prismatic plane as $d_p^{\text{eq}} = 0.05845$, which seems a little close looking at the results...

4.4 TODO Disregistry Analysis

Look into the theory of dissociation distance in Clouet paper [3]

Disregistry given by the Peierls-Nabarro model. Analytic expression given in Hirth and Lothe [4].

Disregistry $D(x)$ is defined as the displacement difference between the atoms in the plane just above and those just below the dislocation glide plane. The derivative of this function $\rho(x) = \partial D / \partial x$ corresponds to the dislocation density.

$$D_{\text{dislo}} = \frac{b}{2\pi} \left\{ \arctan \left[\frac{x - x_0 - d/2}{\zeta} \right] + \arctan \left[\frac{x - x_0 + d/2}{\zeta} + \frac{\pi}{2} \right] \right\}$$

Given x_0 is the dislocation position, d is dissociation length and ζ is the spreading of each partial dislocation.

$$\begin{aligned}
D_L &= \sum_{n=-\infty}^{\infty} D_{\text{dislo}}(x - nL) \\
&= \frac{b}{2\pi} \left\{ \arctan \left[\frac{\tan \left(\frac{\pi}{L} [x - x_0 - d/2] \right)}{\tanh \left(\frac{\pi\zeta}{L} \right)} \right] + \pi \left\lfloor \frac{x - x_0 - d/2}{\zeta} + \frac{1}{2} \right\rfloor \right. \\
&\quad \left. + \arctan \left[\frac{\tan \left(\frac{\pi}{L} [x - x_0 + d/2] \right)}{\tanh \left(\frac{\pi\zeta}{L} \right)} \right] + \pi \left\lfloor \frac{x - x_0 + d/2}{\zeta} + \frac{1}{2} \right\rfloor \right\},
\end{aligned}$$

where $\lfloor \cdot \rfloor$ is the floor function.

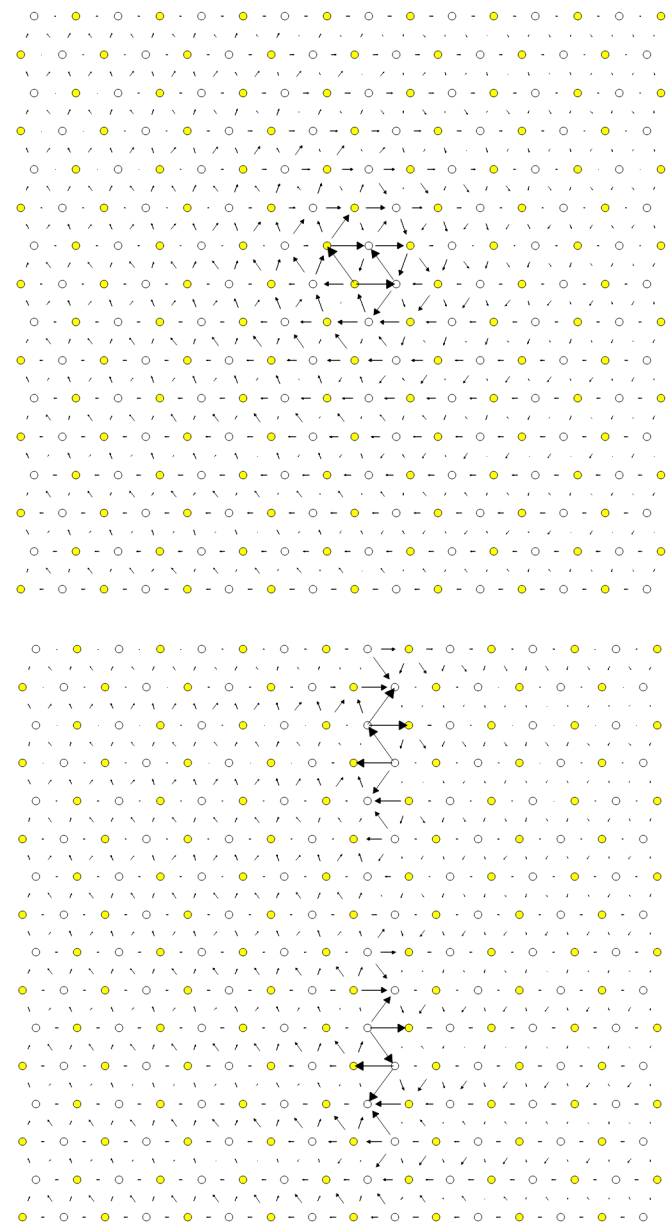
For an array of dislocations in the S arrangement, $D(x) = D_L(x)$, with $L = mc$, where m is the number of repeated unit cells in the U_2 direction.

Here, $U_1 = na\frac{1}{2}[10\bar{1}0]$, $U_2 = mc[0001]$, $U_3 = a\frac{1}{3}[1\bar{2}10]$.

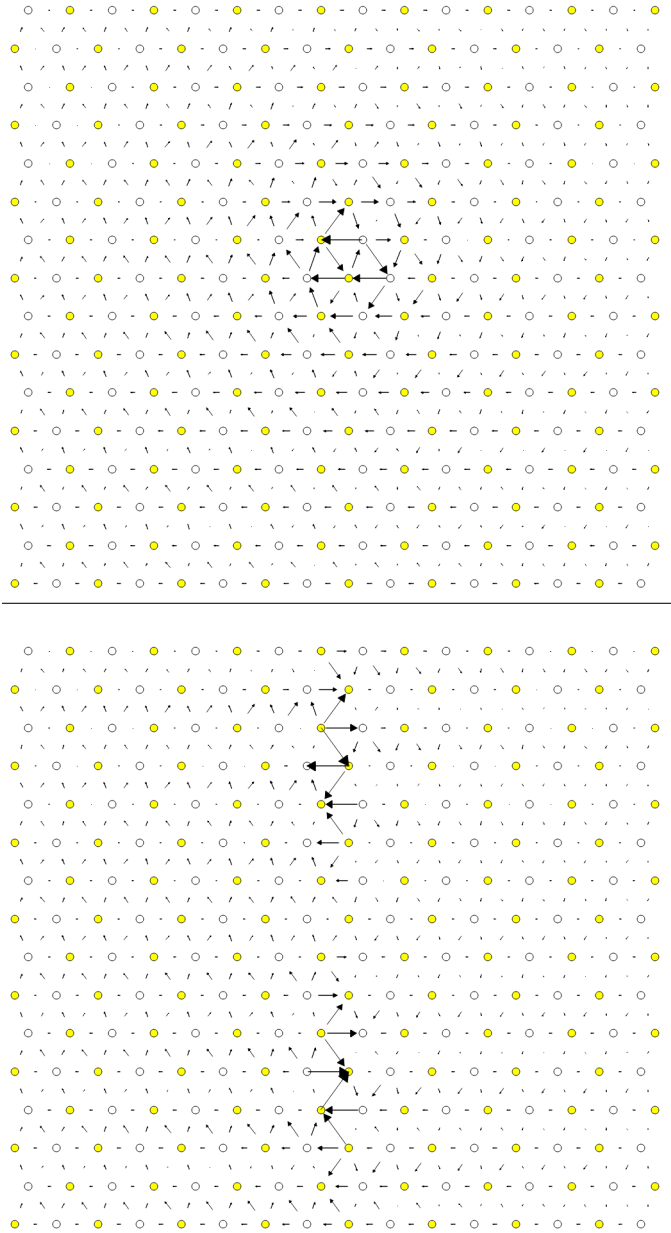
Therefore, using this, one can fit the three fitting parameters: the dislocation position x_0 , the dissociation length d , and the spreading ζ . This procedure therefore allows us to determine the location of the dislocation center.

For all interaction models, we find that this center lies in between two (0001) atomic planes. One can see in Fig. 6 of [3] that this position corresponds to a local symmetry axis of the differential displacement map. This is different from the result obtained by Ghazisaeidi and Trinkle [2] in Ti where the center of the screw dislocation was found to lie exactly in one (0001) atomic plane.

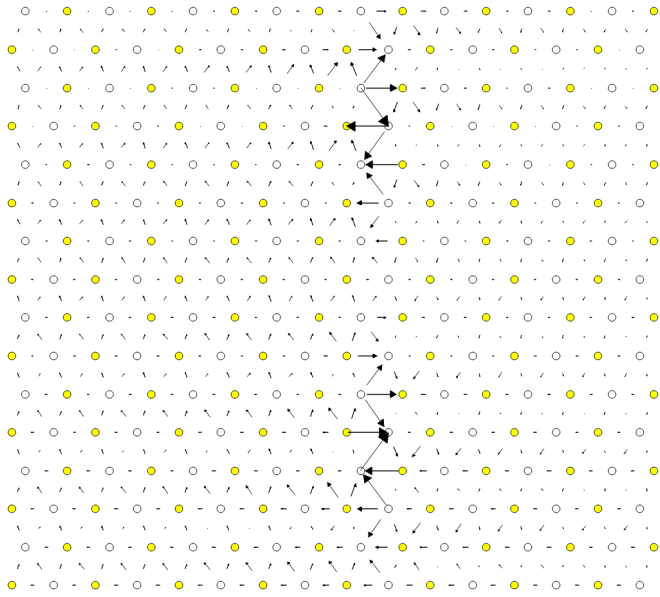
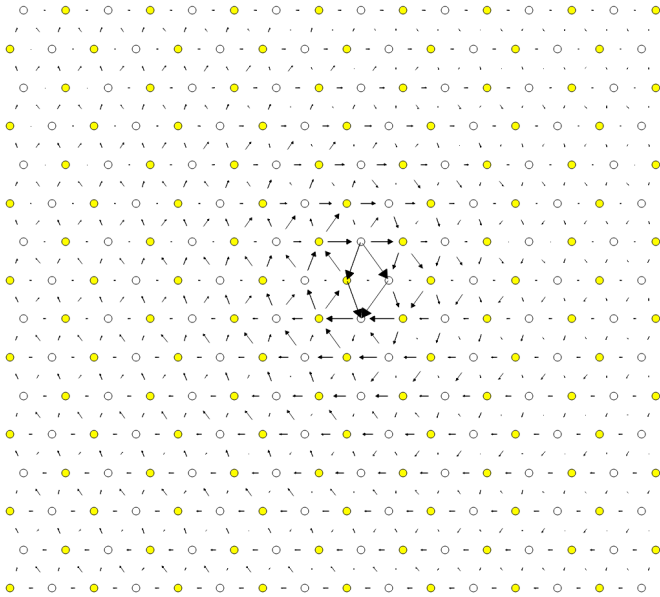
4.5 IP1



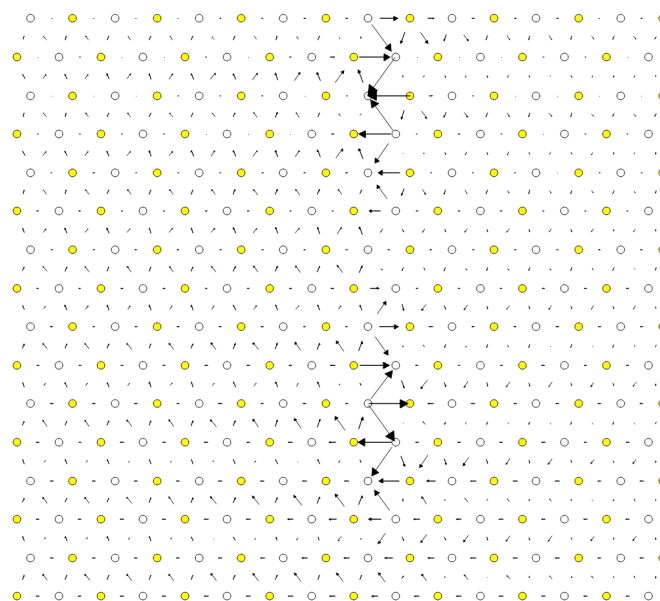
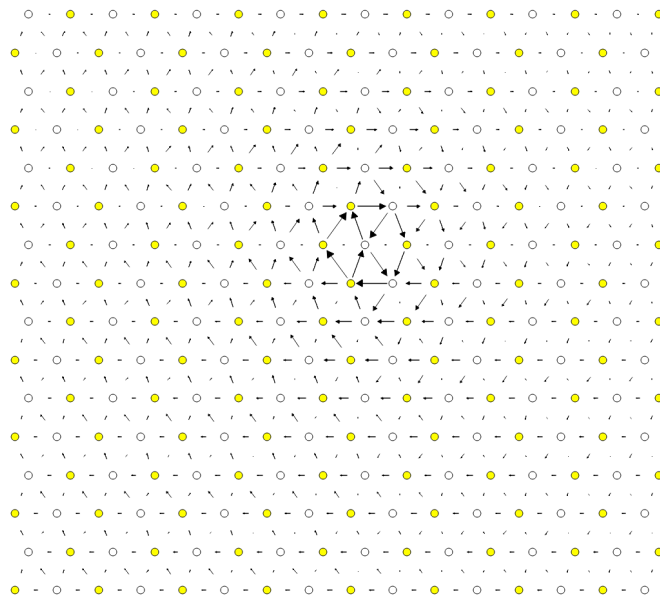
4.6 IP2



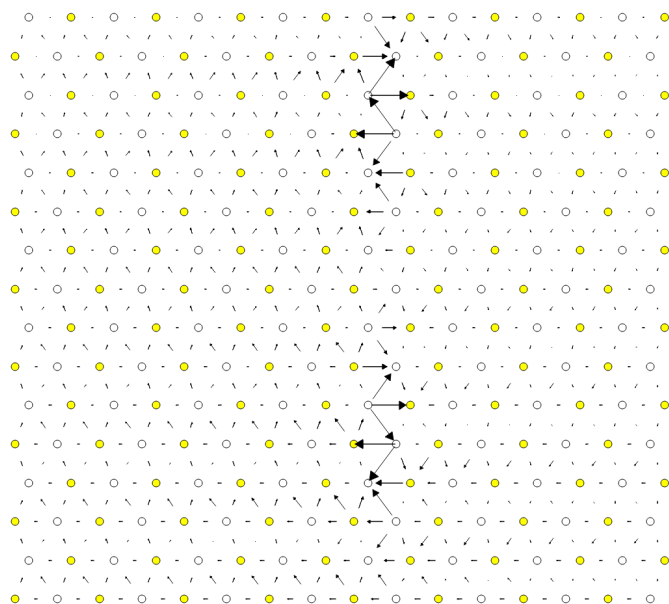
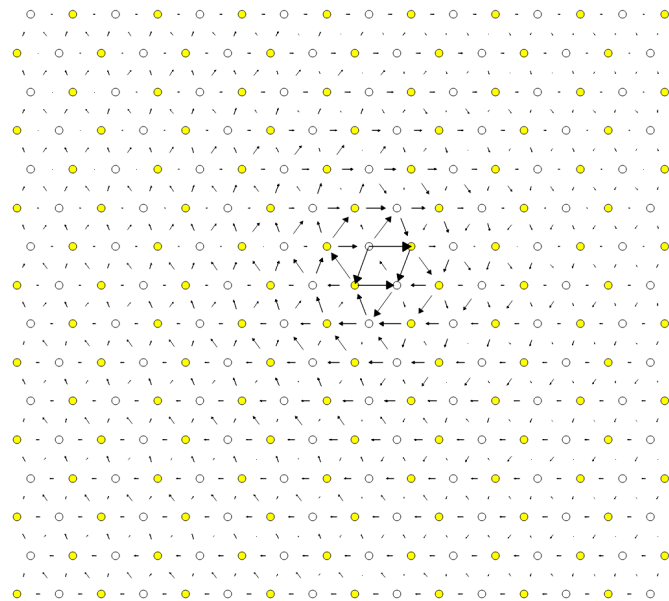
4.7 IP3



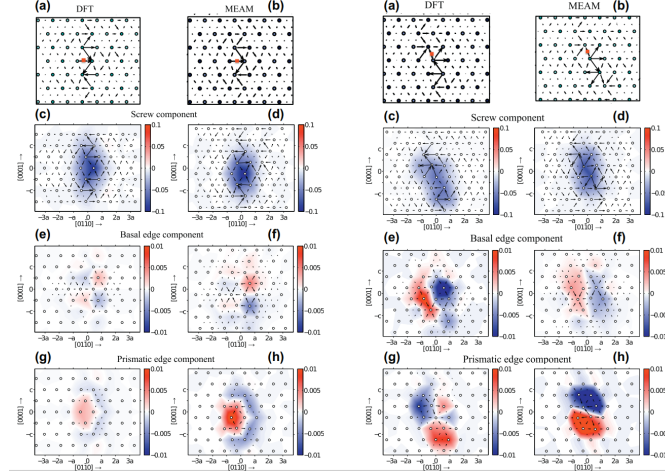
4.8 IP4



4.9 IP5



4.10 Ghazisaeidi Results for comparison



4.11 Peierls Stress

By straining lattice and incrementally increasing the strain, one can find the minimum stress necessary to move a dislocation from one Peierls valley to the next.

4.11.1 Applying strain

Applying strain as in [5].

Here we are incrementing the strain by $0.001C^*$, where C^* is the transformed elastic constant necessary for transforming a strain into a stress from the relation $\sigma_{ij} = C_{ijkl}\varepsilon_{kl}$.

The original elastic constant matrix in its untransformed state is:

$$C = \begin{bmatrix} 171.6093 & 94.6594 & 61.2262 & 0. & 0. & 0. \\ 94.6594 & 171.6093 & 61.2262 & 0. & 0. & 0. \\ 61.2262 & 61.2262 & 198.9006 & 0. & 0. & 0. \\ 0. & 0. & 0. & 47.4255 & 0. & 0. \\ 0. & 0. & 0. & 0. & 47.4255 & 0. \\ 0. & 0. & 0. & 0. & 0. & 38.4749 \end{bmatrix}$$

Transforming it into the dislocation coordinate system, by the rotation

$$C = \begin{bmatrix} 1.0 & 0.0 & 0.0 \\ 0.0 & 0.0 & -1.0 \\ 0.0 & 1.0 & 0.0 \end{bmatrix}$$

$$C^{\text{rot}} = \begin{bmatrix} 171.6093 & 61.2262 & 94.6594 & 0. & 0. & 0. \\ 61.2262 & 198.9006 & 61.2262 & 0. & 0. & 0. \\ 94.6594 & 61.2262 & 171.6093 & 0. & 0. & 0. \\ 0. & 0. & 0. & 47.4255 & 0. & 0. \\ 0. & 0. & 0. & 0. & 38.4749 & 0. \\ 0. & 0. & 0. & 0. & 0. & 47.4255 \end{bmatrix}$$

For finding the Peierls stress to move partials away from each other on the prismatic plane one finds that the stress is given by $\sigma_{xy} = 2C_{xy}^* \varepsilon_{xy}$, where $C_{xy}^* = 47.4255$ GPa.

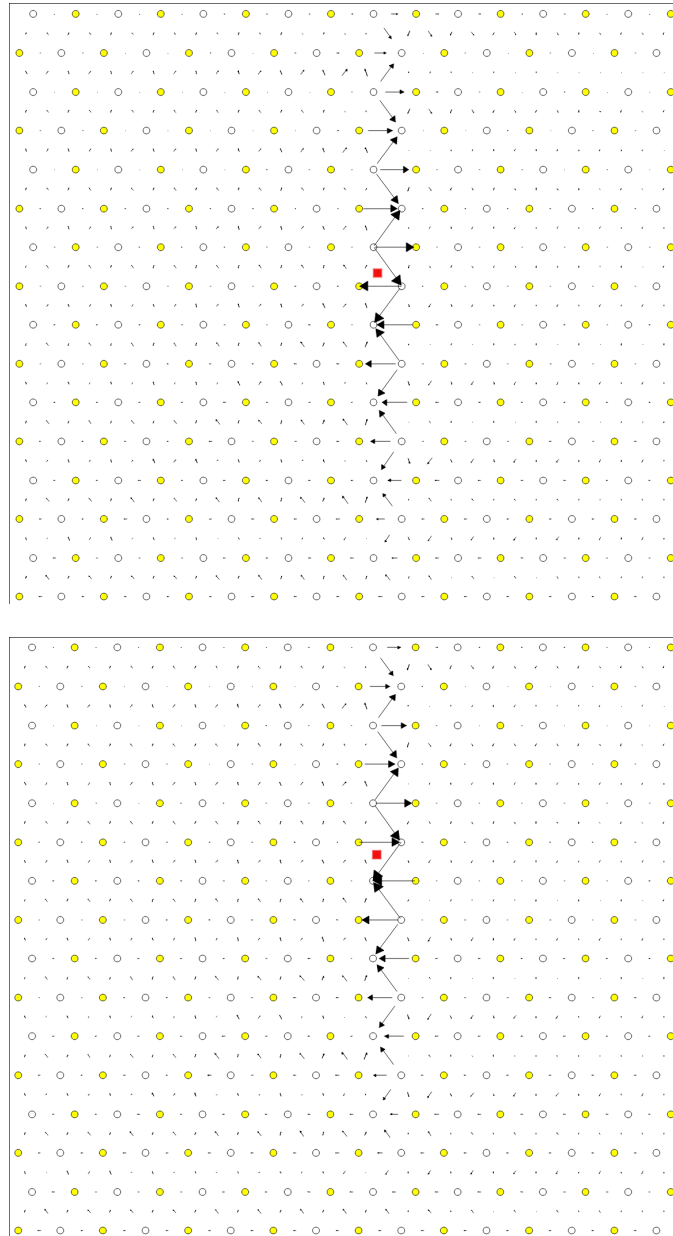
To move the whole dislocation on the prismatic plane, one needs a stress applied which is $\sigma_{xz} = 2C_{xz}^* \varepsilon_{xz}$, $C_{xz}^* = 38.4749$ GPa.

To move the dislocation onto the basal plane one needs to apply a stress given by $\sigma_{yz} = 2C_{yz}^* \varepsilon_{yz}$, $C_{yz}^* = 47.4255$ GPa.

4.11.2 xz Strain

Applying an xz strain to the lattice causes the dislocation to move along the prismatic plane.

Using an increment in the strain of $0.0001C^*$, where C^* is the transformed elastic constant, with a value of $C_{44}^* = 38.4749$ GPa, we find that actually the dislocation moves from one Peierls valley along the prismatic plane at $0.0012C_{44}^*$, giving a Peierls stress of $\sigma_{xz} = 2C_{44}^* \varepsilon_{xz} = 0.0923$ GPa



4.11.3 xy strain

An xy strain can move the partials of the prismatic plane apart.

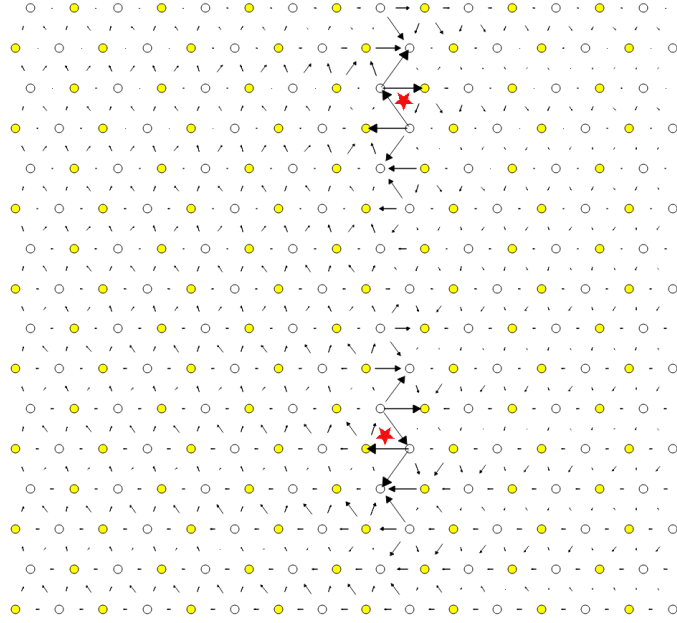
One can find the Peierls stress for these single partials to move in opposite directions.

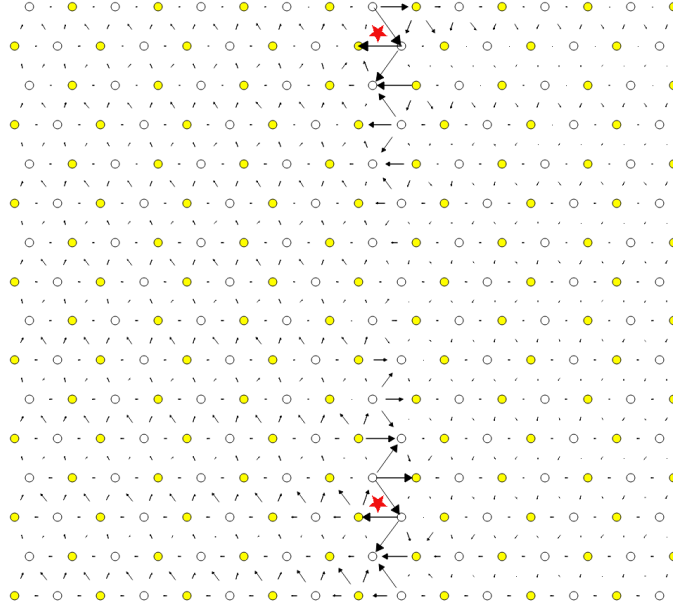
Here the α parameter is 0.03.

This means that the stress necessary to move the partial dislocations apart is

$$\begin{aligned}
 \sigma_{12} &= C_{1212}\varepsilon_{12} \\
 &= 2C_{66}^{\text{Voigt}}\varepsilon_6^{\text{Voigt}} \\
 &= (C_{11} - C_{12})\varepsilon_6^{\text{Voigt}} \\
 &= 47.4255 \times 0.03 \\
 &= 1.42 \text{ GPa}
 \end{aligned}$$

The strain is applied to the whole cell, as the dislocation cell is periodic, then the stress upon each partial is the same.





4.11.4 Pyramidal Strain

For a strain to transform the dislocation into the metastable, pyramidal state, one can apply a strain which applies shear to the dislocation whereby the maximum resolved shear stress is on the first-order pyramidal plane.

In the coordinate system of the dislocation, one finds that the proportions of σ_{xz} and σ_{yz} should be $c/a : \sqrt{3}/2 \approx 1.83 : 1 \approx 1 : 0.54683$.

4.12 Data

IP1 IP2 IP3 IP4 IP5

4.13 Directory of the results

file:///home/tigany/Documents/ti/2019-09-11_final_model/tbe/dislocations/
2019-11-08_no_omega_ordering_ec_latpar/ file:///home/tigany/Documents/
ti/final_model_2019-11

5 Binding energies to dislocations

A strategy to find the binding energies of different sites are to firstly just determine.

1. Octahedral sites near the dislocation core
 - Shall one find a radius within which one can find binding sites?
 - Shall one build the perfect lattice and then move the site into the relaxed octahedral one.
 - Find non-equivalent sites near the core
 - Find the average displacement going from the perfect site to the relaxed cell with dislocation
 - Displace octahedral site by the average of the displacement of the octahedral sites.
2. Relax the relaxed dislocation and the binding sites such that one can find the solution energy.
3. Make perfect lattice, then find displacement from relaxed. Find all octahedral sites near a particular dislocation core and then displace cite by amount

6 BOP

6.1 4 recursion levels

kbT = 0.1

» Lattice parameters:

> hcp

a	2.901660 Å
c	4.747485 Å
etot	-18.342162 eV

> omega

a	7.917318 Å
c	2.749892 Å
etot	-17.458700 eV

Omega is still not as stable as hcp as expected from model.

» Elastic Constants

Quantity	calc. (10^{11} Pa)	exp. (10^{11} GPa)
C11	1.781	1.761
C12	0.738	0.868
C13	0.611	0.682
C33	1.969	1.905
C44	0.285	0.508
C66	0.522	0.450
K	1.050	1.101
R	0.669	0.618
H	0.558	0.489

7 Bibliography

References

- [1] Nathalie Tarrat, Magali Benoit, and Joseph Morillo. Core structure of screw dislocations in hcp ti: an ab initio DFT study. *International Journal of Materials Research*, 100(3):329–332, mar 2009.
- [2] M. Ghazisaeidi and D.R. Trinkle. Core structure of a screw dislocation in ti from density functional theory and classical potentials. *Acta Materialia*, 60(3):1287–1292, feb 2012.
- [3] Emmanuel Clouet. Screw dislocation in zirconium: An ab initio study. *Physical Review B - Condensed Matter and Materials Physics*, 86(14):1–11, 2012.
- [4] P.M. Anderson, J.P. Hirth, and J. Lothe. *Theory of Dislocations*. Cambridge University Press, 2017.
- [5] Z M Chen, M Mrovec, and P Gumbsch. Atomistic aspects of $\langle 111 \rangle$ screw dislocation behavior in-iron and the derivation of microscopic yield criterion. *Modelling and Simulation in Materials Science and Engineering*, 21(5):055023, June 2013.